BRAIN CONNECTIVITY
Volume 3, Number 3, 2013

DOI: 10.1089/brain.2012.0119

Dynamic Coupling Between the Lateral Occipital-Cortex, Default-Mode, and Frontoparietal Networks During Bistable Perception

Ariel Karten,[1–3,*] Spiro P. Pantazatos,[1,4,*] David Khalil,[5] Xian Zhang,[1,6] and Joy Hirsch[1,6–8]

Abstract

The lateral occipital cortex (LOC), a visual area known to be involved in object recognition, was dynamically coupled with each of two distributed patterns of neural activity depending upon the percept (default or alternative) elicited by a bistable figure. The two distributed patterns included core nodes of the default-mode and frontoparietal networks (FPN), and they were most highly coupled to each other during the alternative percept, whereas they were less coupled during the default percept. Surprisingly, the regions associated with the nonengaged percept exhibited the highest connectivity to the LOC. Together, these findings reveal a dynamic organization between the default mode and the FPNs, and the incoming bottom-up visual stream during perceptual binding of visual images.

Key words: default mode network (DMN), frontoparietal network (FPN), functional connectivity, functional magnetic resonance imaging (fMRI), image segmentation, neural suppression, psychophysiological interactions (PPI), visual perception

Introduction

The mechanism by which the neural correlates of human vision segment and bind features to form unified percepts from a complex visual world is a long-standing central question that has also been linked to more general questions related to the neural correlates of awareness and consciousness (Leopold and Logothetis, 1999; Rees et al., 2002; Sterzer et al., 2009). Image segmentation is a complex process by which stimulus elements are perceptually arranged into a unified whole. A bistable figure presents a unique opportunity to investigate mechanisms involved in segmentation of visual input, because one stimulus elicits two mutually exclusive percepts representing alternative organizations of the same visual input. Although neuroimaging studies have previously confirmed the involvement of the parietal and frontal brain regions in high-level visual processes, including bistable perception (Kleinschmidt et al., 1998), there is no established framework to describe the underlying neural mechanisms of image segmentation. We envision that this complex process of alternating visual perceptions will employ large-scale distributed neural systems.

The default-mode network (DMN), sometimes referred to as the task-negative network, has been defined by task-induced deactivations as well as higher energy consumption during rest, and consists of temporal and midline structures that are known to be more active during rest than during a task (Buckner et al., 2008; Greicius et al., 2003; Gusnard et al., 2001; Raichle et al., 2001). It has also been associated with internal stimuli or self-reflection as well as memory of past events (Andrews-Hanna et al., 2010). The frontoparietal network (FPN), sometimes referred to as the task-positive network, is classically defined by task-induced activations, and consists of the dorsal, frontal, and parietal regions associated with volitional tasks that require attention to external stimuli (Corbetta and Shulman, 2002; Dosenbach et al., 2007; Kastner and Ungerleider, 2000). These two networks have also been identified on the basis of spontaneous correlations during resting states characterized by anticorrelations between them (Anderson et al., 2011; Fox et al., 2005),

[1]Functional MRI Research Laboratory, Columbia University College of Physicians and Surgeons, New York, New York.
[2]Macaulay Honors College, City University of New York, New York, New York.
[3]Departments of Biology and Psychology, City College of New York, City University of New York, New York, New York.
[4]Department of Physiology and Cellular Biophysics, Columbia University College of Physicians and Surgeons, New York, New York.
[5]Department of Dermatology, Yale University School of Medicine, New Haven, Connecticut.
[6]Department of Psychology, Columbia University, New York, New York.
Departments of [7]Radiology and [8]Neuroscience, Columbia University College of Physicians and Surgeons, New York, New York.
*These authors contributed equally to this manuscript and should be viewed as co-first authors.

suggesting an intrinsic oppositional functional organization of neural processes that mediate cognitive tasks. Despite a general consensus regarding the regions comprising these networks, there is a lack of consensus regarding their functions.

In this study, functional magnetic resonance imaging (fMRI) and functional connectivity methods were employed to identify neural substrates and dynamics engaged during each of the mutually exclusive percepts elicited by a common bistable figure, the Schröder Staircase (Schröder, 1858). Subjects viewed alternating 15-sec blocks of rest and stimulus, and were instructed on each stimulus block that percept to maintain, that is, default or alternative. All subjects were well practiced, and they demonstrated competence with the task before scanning. This paradigm differs from previous studies of bistable perception (Kleinschmidt et al., 1998; Tong et al., 1998) by providing a targeted percept with instructions to maintain a percept for each 15-sec block. This paradigm was chosen to provide a structured focus on each percept, which permitted an experimental approach to investigate the underlying neural circuitry associated with each percept.

In the default condition, the figure was readily perceived as a familiar staircase, whereas in the alternative condition, the figure was perceived as an inverted staircase. Although prior investigations of bistable perception have considered the role that attention plays in forming each of the percepts (Meng and Tong, 2004; Slotnick and Yantis, 2005), the attention network and its relation to the DMN have not been previously implicated in this process. As is typical with bistable figures, the two percepts differed with respect to the volitional effort and attention required for their realization, suggesting a putative role for both the attentional control and the DMNs. In this study, we test the hypothesis that mutually exclusive visual image segmentations, as in the case of two bistable percepts, are associated with neural processes that engage both the default-mode and the frontoparietal attention networks. Further, we compare the coupling between the networks and the bottom-up visual stream during the two perceptual states to investigate the intrinsic dynamic organization associated with these percepts.

Materials and Methods

Subjects

A total of 12 healthy volunteers participated in the functional imaging study (8 men and 4 women; ages 18–27 years of age; mean = 22.8 years of age), as approved by the institutional review board of the Columbia University Medical Center. All subjects were informed about possible risks of MRI and provided consent according to the established guidelines.

Stimulus

The stimulus was a black-and-white line drawing of a common bistable figure (Supplementary Fig. S1; Supplementary Data are available online at www.liebertpub.com/brain) referred to as the Schröder Staircase. The two percepts were mutually exclusive, and the eye position monitoring has previously provided no evidence for percept-associated variations (Hirsch et al., 2004).

Functional imaging procedures

The functional study was run as a block design in which the stimulus was presented for 12 fifteen-sec epochs, each of which was preceded by a 15-sec baseline epoch that featured a black screen with a crosshair (+). Before scanning, the default and the alternative percepts were determined for each subject based on the percept that the subject reported as seen first and most automatically. For all subjects, the default percept was the ascending staircase most resembling a familiar staircase, and the alternative percept was the upside-down staircase that appeared to be suspended in midair. The subject was instructed to hold the default percept for the first 15-sec stimulus epoch, and then, following a rest epoch, instructed to hold the alternative percept for the following 15-sec stimulus epoch, and to continue this alternation for the duration of the 6.0-min run. The target percepts were cued by the written words alternative or default above the image, and the subjects indicated on a keypad the actual engaged percept and whenever a perceptual switch (voluntary or otherwise) occurred. Subjects practiced outside the scanner until they could perform this perceptual task. Button-press indications of the engaged percept confirmed that on average, the default percept was sustained for a total of 92.36 ± 6.48 sec, whereas the alternative percept was sustained for a total of 75.7 ± 6.16 sec, and are consistent with known difficulty and attentional differences between the two percepts. The average total time that the default percept occurred spontaneously during the target alternative condition was 20.34 ± 6.29 sec, whereas the average total time that the alternative percept occurred spontaneously during the target default condition was 12.01 ± 4.92 sec, and also consistent with the default percept as the more natural and less effortful of the two.

Image acquisition and analysis

Functional images were acquired on a 1.5T GE MRI scanner located in the Columbia University fMRI Research Center, New York, NY. Whole-brain eco planar functional images (EPI) were collected with an 8-channel GE head coil in 25 contiguous axial slices obtained parallel to the AC/PC line (TR = 3000 ms, TE = 35 ms, flip angle = 84 degrees, FoV = 19.2×19.2 cm^2, array size = 128×128, spatial resolution of acquisition = $1.5 \times 1.5 \times 4.5$ mm, voxel size after spatial normalization = $2 \times 2 \times 2$ mm). One hundred twenty whole-brain images were acquired during each of two identical 6-min runs. High-resolution 3-D anatomical scans were also acquired with a T1-weighed SPGR sequence (TR = 19 ms, TE = 5 ms, flip angle = 20 degrees) FoV = 220×200 mm, a slice thickness of 1.5 mm, in-plane resolution of 0.86×0.86 mm, and 124 slices per image.

Image preprocessing and statistical analysis were completed using SPM8 software (Wellcome Department of Cognitive Neurology, University College London, UK). Functional T2*-images were slice-timing corrected and spatially realigned to the first volume of the first run. Finally, images were smoothed with a Gaussian kernel of $8.0 \times 8.0 \times 8.0$-mm full-width half-maximum, and a 128-s temporal high-pass filter was applied.

General linear model analysis

Statistical analysis of the blood oxygen level-dependent (BOLD) signal was modeled using a single-factor percept,

with two levels: alternative and default. The analysis aimed to detect activity associated with each perspective. Perceptual durations (according to button presses) for the default and alternative percepts were convolved with the canonical hemodynamic response function (HRF). Additional nuisance regressors, that is, six motion parameters, mean white-matter, and mean CSF signal, were included to remove unnecessary noise from the data. Contrasts of resulting beta-estimates (Default > Alternative and Alternative > Default) for each run separately were averaged across both runs, and were passed to 2nd-level random-effect analyses (one-sample *t*-tests). Beta-estimates from each condition were also passed to a 2nd-level random-effect analysis (paired *t*-test) to determine conjoined activation and deactivation common to both percepts in run 1, used for independent region of interest (ROI) analyses (see below).

Psychophysiological interaction analysis

The psychophysiological interaction (PPI) analysis measures the extent to which regions are differentially correlated between conditions (Friston et al., 1997), and is strictly correlative and not indicative of directional causation. While there are various approaches regarding the removal of task-associated variance in PPI analysis (McLaren et al., 2012; O'Reilly et al., 2012), we have adopted the long-standing standard approach as described in the current version of SPM8 (www.fil.ion.ucl.ac.uk/spm/doc/manual.pdf). Lateral occipital cortex (LOC), the primary seed of interest, was defined by averaging the time series of the right and left LOC, thus merging them into one single bilateral seed. Bilateral LOC was defined by the conjunction of alternative and default activity, at peak MNI coordinates for right [40-70-8] and left [-38, -78-6], thresholded at $p < 0.0001$, uncorrected corresponding to the LOC, which has been shown to be active in object recognition (Grill-Spector et al., 2001; Malach et al., 1995). Similarly, composite DMN and FPN seeds were defined using the conjunction of both default and alternative conditions from Run 1. Positive contrast of the conjunction was used to identify the FPN seed, and negative contrast was used to identify the DMN seed. All ROIs in a given network were then joined using the Marsbar Toolbox (http://

Table 1A. Areas Active During the Default Percept as Defined by the Contrast Default > Alternative and Also Identified as Elements of the Default-Mode Network

Default > Alternative Contrast (DMN)						
GLM region		*x*	*y*	*z*	*t-value*	*Cluster size*
Middle temporal cortex	*mTC (L)	−58	−36	−4	4.60	1939
	mTC (R)	54	−40	−2	4.42	1195
Anterior cingulate cortex	ACC	−2	24	−4	5.24	765
Posterior cingulate cortex	PCC	−8	−36	32	3.02	584
Inferior parietal lobule	*IPL (L)	−44	−64	40	4.38	1510
	IPL (R)	54	−64	40	3.31	347
Medial prefrontal cortex	*MPFC	4	46	44	4.95	2486
Lateral prefrontal cortex	*LPFC	12	38	46	5.90	2488
Precuneus	PC	−6	−56	52	3.59	1462

ROI abbreviations, peak voxel MNI coordinates (*x*, *y*, *z*), *t*-values, and cluster sizes are shown for each region.
Asterisks indicate the regions that survive cluster correction thresholding at $p < 0.005$ and a cluster size of 150.
DMN, default-mode network; GLM, general linear model.

Table 1B. Areas Active During the Alternative Percept as Defined by the Contrast Alternative > Default and Also Identified as Elements of the Frontoparietal Network

Alternative > Default Contrast (FPN)						
GLM region		*x*	*y*	*z*	*t-value*	*Cluster size*
Lateral occipital cortex	LOC (L)	−46	−58	−8	3.80	642
	LOC (R)	40	−78	−12	5.83	448
Middle occipital cortex	mOC (L)	−26	−88	6	3.85	188
	mOC (R)	20	−98	10	2.87	358
Inferior frontal cortex	IFC	46	8	26	4.43	733
	IPL (L)	−46	−34	50	6.68	597
Inferior parietal cortex	IPL (R)	20	−52	50	4.85	313
	IPL (R)	48	−38	46	3.74	280
Superior parietal cortex	SPL (L)	−18	−68	52	3.48	126
	SPL (R)	16	−76	52	3.14	241
Middle frontal gyrus	mFG (L)	−32	−10	50	4.84	382
	mFG (R)	24	−4	52	5.07	281
Supplementary motor area	SMA	−4	6	52	5.20	986

ROI abbreviations, peak voxel MNI coordinates (*x*, *y*, *z*), *t*-values, and cluster sizes are shown for each region.
FPN, frontoparietal network.

marsbar.sourceforge.net/) to form a single composite network seed thresholded at $p < 0.0001$ (Uddin et al., 2009). The BOLD time courses were extracted from two 6-mm spheres each centered at the above coordinate locations, respectively, and then regressed on a voxel-wise basis against the product of this time course and the vector of the psychological variable of interest, (1*Default + −1*Alternative), with the physiological and the aforementioned psychological variable (a regressor convolved with the HRF representing the contrast default > alternative) serving as regressors of no interest. The resulting beta-maps were subsequently passed to 2nd-level random-effect analysis (one-sample *t*-test). Results for the left and right seeds were similar; hence, reported results are based on the combined bilateral seed. General linear models (GLM) models that were used to extract the seed region activity and to estimate PPI results included additional nuisance regressors, that is, six motion parameters, mean white-matter, and mean CSF signal. For display purposes, statistical maps were thresholded at $p < 0.05$ uncorrected. To control for multiple comparisons throughout the brain, cluster-extent thresholding was applied using an uncorrected cutoff *p*-value of 0.005 and a cluster size threshold of 150 contiguous voxels resulting in an effective $p < 0.05$ corrected (denoted by an asterisk in Table 1A and 1B). This cluster threshold was determined by 2000 Monte Carlo simulations of whole-brain fMRI data with respective parameters of the presented study (Gaussian kernel = 8 × 8 × 8 mm, voxel size = 2 × 2 × 2 mm, mask = whole-brain fMRI data) using AlphaSim in AFNI (v2009).

Independent ROI analysis

To test whether the DMN and FPN were significantly more active and functionally connected with the visual cortex during one percept versus the other, we conducted an independent ROI analysis using the Marsbar Toolbox (http://marsbar.sourceforge.net/). For this, the FPN and DMN were defined using conjunction of both the default and alternative conditions from Run 1 of each subject. These beta-estimates were input to a 2nd-level random-effect analysis (2-sample *t*-test) in which positive and negative conjunction contrasts, thresholded at $p < 0.0001$, uncorrected, defined the independent FPN and DMN ROIs (Uddin et al., 2009). Contrast values (or beta-estimates from PPI analyses) of Default-Alternative from Run 2 of each subject were then averaged over all voxels within the above ROIs, and submitted to two separate 2nd-level random-effect analysis (one-sample *t*-tests, one for each ROI).

Effective connectivity analysis

Effective connectivity analysis was carried out using dynamic causal modeling, DCM (Friston et al., 2003), as implemented in SPM8 (Wellcome Department of Cognitive Neurology, University College London, UK). Predictions based on the observed data consist of the combination of driving inputs, intrinsic connection activity, and bilinear modulation, which reflects the effects of experimental variables. In this case, the default and alternative percept conditions served as both the driving input (on individual regions) and the modulatory input (on connections between regions). These effects are modeled by the equation, $dz_1/dt = (A + u_mB)z_2 + Cu_i$, in which dz_1/dt is the state vector per unit time for the target region; z_2 corresponds to timeseries data from the source region; u_i indicates the direct input to the model; and u_m indicates input from the modulatory variable onto intrinsic pathways specified by the model. Activity in the target region is therefore determined by an additive effect of the intrinsic connectivity with the source region (Az_2), the bilinear variable (u_mBz_2, corresponding to the modulatory experimental manipulation), and the effect of direct input into the model (Cu_i).

Given our specific hypotheses, a fully specified model was estimated (i.e., intrinsic bilateral connections between the LOC, DMN, and FPN, with both conditions modulating all regions and connections). In each subject, the contrast (Default > Alternative) was calculated for each connectivity parameter and submitted to a one-sample *t*-test over all the subjects. Unless otherwise indicated, there were 11 degrees of freedom for all reported t-values.

Results

Functional magnetic resonance imaging

Patterns of whole-brain fMRI activity based on the BOLD response observed during the default > alternative contrast (Fig. 1a) and alternative > default contrast (Fig. 1b) corresponded to known activity patterns previously associated with the DMN (Anderson et al., 2011; Buckner et al., 2008; Greicius et al., 2003; Raichle et al., 2001) and FPN (Anderson et al., 2011; Corbetta and Shulman, 2002; Dosenbach et al., 2007; Kastner and Ungerleider, 2000), respectively. In particular, the default perspective activity (as defined by the contrast default > alternative; Table 1A) included the middle temporal cortex, anterior cingulate cortex, posterior cingulate cortex, inferior parietal lobule (IPL), medial prefrontal cortex, lateral prefrontal cortex, and precuneus (PC), which have been previously associated with the DMN (Buckner et al., 2008; Greicius et al., 2003; Raichle et al., 2001). In comparison, the alternative perspective activity (as defined by the contrast alternative > default; Table 1B) included the LOC, middle occipital cortex, inferior frontal cortex, IPL, superior parietal lobule, middle frontal gyrus, and supplementary motor area, which have previously been associated with the FPN (Corbetta and Shulman, 2002; Dosenbach et al., 2007; Kastner and Ungerleider, 2000). An independent ROI analysis confirmed that activation of the DMN, as a whole, was significantly greater during the default perspective (default > alternative, $t = 2.29$, $p < 0.05$), while activation of the FPN, as a whole, was significantly greater during the alternative perspective (alternative > default, $t = 2.01$, $p < 0.05$) (see the Materials and Methods section).

Functional connectivity with the LOC

The functional roles of the DMN and FPN in bistable image segmentation were explored in relation to the incoming bottom-up visual stream. PPI analysis of functional connectivity between the LOC, which was active during both percepts, and all other brain regions revealed that a higher connectivity was observed between the LOC and the network associated with the unconscious percept. For example, during the default percept (default > alternative contrast), LOC connectivity increased specifically with the FPN regions (Fig. 2a), whereas connectivity during the alternative percept

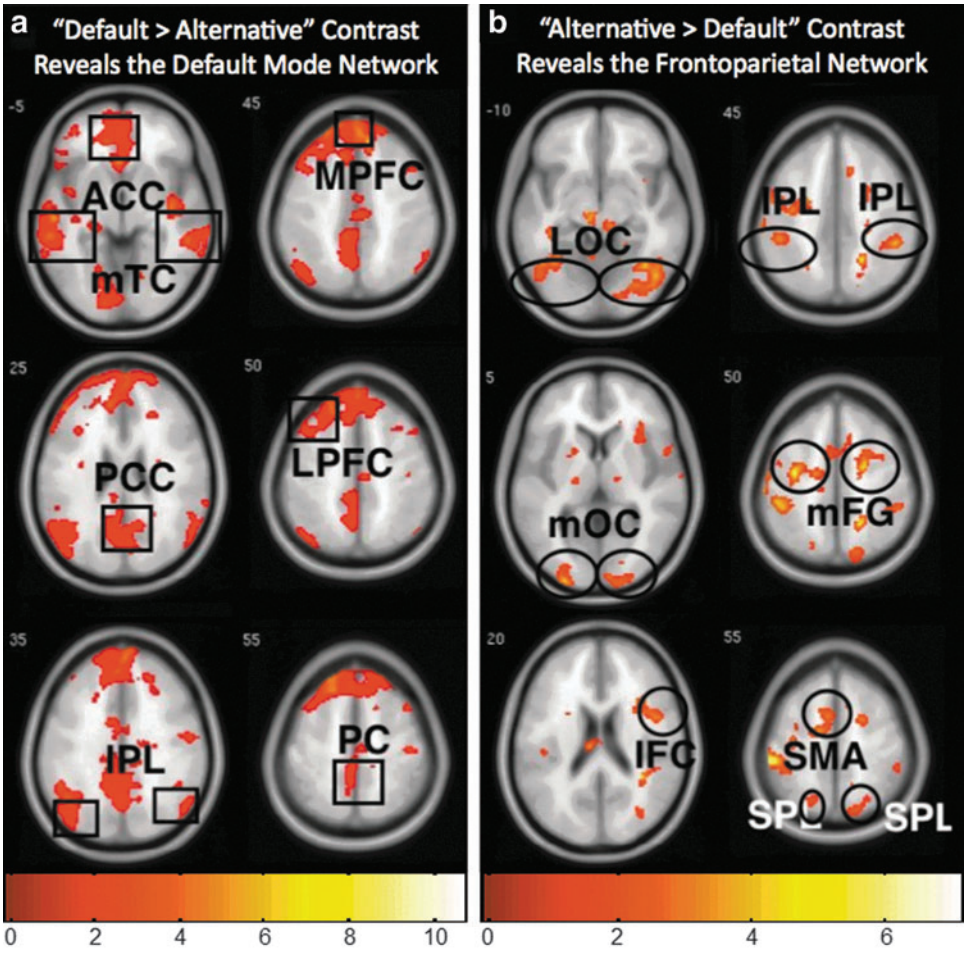

FIG. 1. **(a)** Blood oxygen level-dependent (BOLD)-related functional magnetic resonance imaging (fMRI) activity associated with the default percept as defined by the contrast default > alternative. The boxed clusters indicate regions previously identified as part of the default-mode network (DMN). **(b)** fMRI activity associated with the alternative percept as defined by the contrast alternative > default. The circled clusters indicate the regions previously identified as the frontoparietal network (FPN). Images are shown on a normalized brain with slice positions in mm from the AC/PC line indicated on the upper left. For display purposes, maps are thresholded at $p < 0.05$, $k = 10$.

(alternative > default contrast) increased specifically with the DMN regions (Fig. 2b). An independent ROI analysis confirmed that connectivity with the FPN was significantly greater during the default perspective (default > alternative, $t = 4.80$, $p < 0.05$), while connectivity with the DMN was greater during the alternative perspective (alternative > default, $t = 5.39$, $p < 0.05$) (see the materials and Methods section).

Connectivity between the FPN and DMN

In addition to the dynamic connectivity between the LOC and the two networks, the connectivity between the DMN and FPN was also measured using PPI analysis to investigate possible cross-network connectivity in association with connectivity with the incoming visual stream. During the default contrast, both the DMN (Supplementary Fig. S2a) and the FPN (Supplementary Fig. S2b) exhibited higher connectivity within their respective networks. Independent ROI analyses confirmed that the connectivity within each network was significantly greater during the default perspective (default > alternative, DMN $t = 4.45$, $p < 0.05$ and FPN $t = 6.58$, $p < 0.05$). During the alternative contrast, however, the two networks increased their connectivity to each other, such that the DMN was more connected to the FPN (Supplementary Fig. S3a), and the FPN was more connected to the DMN (Supplementary Fig. S3b) as shown by the PPI results. This cross-network connectivity that was observed most prominently during the alternative perspective was also confirmed by independent ROI analyses (alternative > default, DMN connectivity with FPN seed, $t = 3.63$, $p < 0.05$ and FPN connectivity with DMN seed $t = 5.33$, $p < 0.05$). In general, the PPI analysis indicates that during the default contrast, the individual networks tended to be more connected within themselves, whereas during the alternative percept, the cross-network functional connectivity was increased.

Effective connectivity

The PPI findings were also confirmed by a dynamic causal model (Penny et al., 2004), where effective connectivity between the LOC, DMN, and FPN was estimated during both conditions using a fully specified model. In accordance with our model, significant contrasts of connectivity parameters (Alternative > Default) were observed for the connectivity from the DMN to the LOC ($t = 1.91$ and $p < 0.04$), and from the FPN to the DMN ($t = 1.79$ and $p < 0.05$). Thus, these two approaches, PPI and DCM, provide convergent findings, indicating that during the alternative percept, the connection was increased between the LOC and the DMN, and also between the FPN and DMN.

Discussion

Differences in connectivity between the cortical regions have previously been reported depending upon volitional (top-down) goals (Chadick and Gazzaley, 2011), as well as

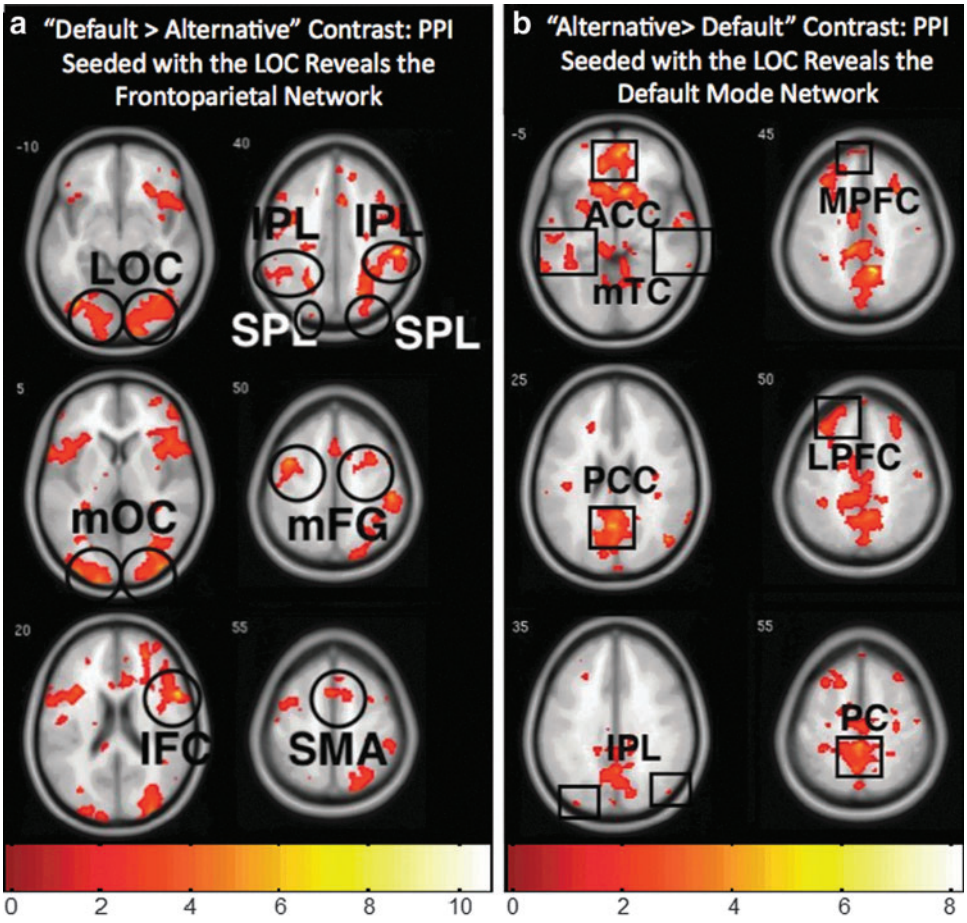

FIG. 2. Functional connectivity (PPI) between the lateral occipital cortex (LOC) and regions where connectivity during one percept (as defined by the contrasts) exceeds connectivity in comparison to the other. The same global networks observed in the fMRI analysis (Fig 1) were also observed in the PPI analysis, however, **(a)** the connectivity pattern from the LOC is highest to FPN regions during the default-percept contrast, and **(b)** the connectivity pattern from the LOC during the alternative-percept contrast is highest to the DMN regions. For both figures **(a)** and **(b)**, group results are shown on a normalized brain with slice positions in mm from the AC/PC line indicated on the upper left. For display purposes, maps were thresholded at $p < 0.05$, $k = 10$.

interactions between the DMN and the FPN (Fox et al., 2005; Uddin et al., 2009). Here we extend these findings and show that volitional image segmentation tasks also engage distributed neural patterns consistent with the DMN and the FPN. Further, functional connectivity reveals a mechanism of oppositional coupling and decoupling between the incoming visual stream and these networks that is associated with the bistable percepts.

Recent EEG findings reporting that neural activity precedes the perceptual emergence of the hidden percept (Britz et al., 2009) are consistent with our finding that the nonengaged percept is associated with an active process correlated with the incoming visual stream. Further, previously proposed models for bistable perception suggest that fatigue or satiation of the neural correlates associated with conscious percept contribute to the emergence of the suppressed

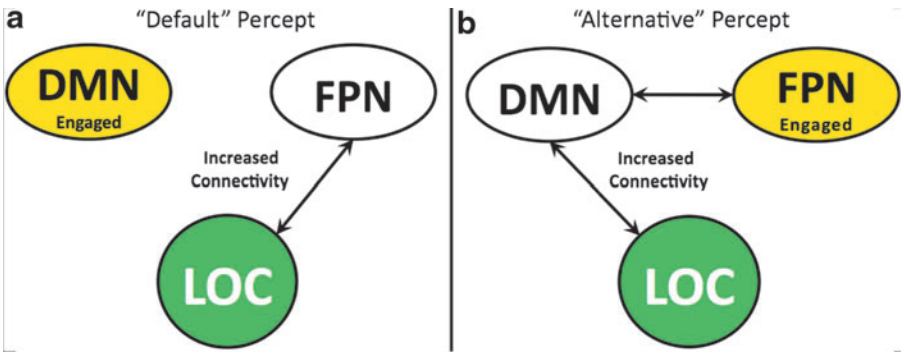

FIG. 3. A conceptual summary of findings. **(a)** During the conscious default percept, as revealed by the default > alternative contrast, the DMN was more engaged, and the functional connectivity increased between the LOC and the FPN. There was no evidence for cross network connectivity during this percept. **(b)** During the conscious alternative percept, as revealed by the alternative > default contrast, the FPN was more engaged, and the functional connectivity increased between the LOC and the DMN. Additionally, functional connectivity between the FPN and DMN was observed in this condition.

percept (Toppino and Long, 1987). Our data are also consistent with the notion that active stages of percept construction involve neuronal suppression between the levels of visual information processing. For example, our finding that the DMN and the FPN are more internally correlated during the default percept, that is, increased intranetwork connectivity, and more cross-correlated during the alternative, that is, increased internetwork connectivity, is consistent with the previously reported competitive and suppressive interactions between these networks (Kelly et al., 2008; Uddin et al., 2009).

A framework proposed by (Spreng et al., 2010) can be applied to our findings where a model of interactive top-down neural processes originating from the FPN mediates between the two networks (Fig. 3). During the default percept, the distributed BOLD response was consistent with DMN activity (the DMN was less deactivated during the default percept relative to the alternative percept), whereas during the alternative percept, the distributed BOLD response was consistent with FPN activity, indicating that when one network was active (Fig. 3- yellow), the other was relatively less active.

The functional connectivity between the bottom-up visual stream, originating from the LOC (Fig. 3–green), was highly correlated with the less-engaged network. Variations in concurrent deactivations of irrelevant sensory input have been associated with a suppressive mechanism (Amedi et al., 2005; Shmuel et al., 2002; Wade, 2002). Accordingly, our finding of the increased connectivity between the FPN and the deactivated DMN suggests that the FPN may suppress DMN activity during the alternative percept. Additionally, during the default percept, the less-engaged FPN was internally connected suggestive of a regulation of this suppressive mechanism. These findings lead to the novel interpretation that increased connectivity between the visual stream and the deactivated network reveals a suppressive mechanism associated with the conscious percept possibly mediated by oppositional long-range networks that interact with the incoming visual information (Fig. 3).

The discovery that the bottom-up visual stream was anticorrelated with the network associated with the ongoing conscious percept is surprising. However, working with the framework put forth, these new findings can be interpreted as reflecting a balance between the suppressive and excitatory interactions between the networks that are associated with the unconscious and conscious percepts and the bottom-up visual stream. Together, these findings are consistent with a model where active image segmentation, as observed in bistable figures, is mediated by top-down mechanisms that influence incoming visual information.

Conclusion

Bistable percepts provide a unique opportunity to investigate the neural mechanism of image segmentation, because a single visual figure gives rise to two mutually exclusive perceptual constructs. In this study, percepts elicited by the Schroder Staircase differentially gave rise to distributed patterns of neural activity consistent with the DMN and an FPN, during fMRI. In particular, the DMN was observed during the default percept, while the FPN was observed during the alternative percept. Additionally, the functional connectivity revealed that the incoming visual stream was more coupled with the DMN during the more effortful, alternative percept, and that the DMN and FPN were most interconnected during the alternative percept. These findings suggest that the process of binding image segments into perceptual units engages oppositional and interacting long-range neural networks.

Author Contributions

JH supervised the study. AK and DK performed the experiments. AK analyzed the activation data. SPP analyzed the functional connectivity data. JH and AK drafted the manuscript. XZ assisted with data analysis and provided technical advice.

Acknowledgments

Authors are grateful for significant contributions by students and subjects who have participated in the development of this project, including Grace Lai (Columbia University Program in Neuroscience), graduate and undergraduate educational support for science education, Macaulay Honors College [AK], and the Intel Science Competition for high school students [AK, DK]. Current funding for this project includes *NIAAA-09-07* (NIH) HHSN27500900019C (subcontract to JH, PI Jon Morgenstern); a predoctoral fellowship (NRSA) F31MH088104-02 (SP, mentor: JH); U.S. Army RDECOM-TARDEC W56H2V-04-P-L (JH); and NIH RO1NS056274 (subcontract to JH, PI Nicholas Schiff).

Author Disclosure Statement

No competing financial interests exist.

References

Amedi A, Malach R, Pascual-Leone A. 2005. Negative BOLD differentiates visual imagery and perception. Neuron 48:859–872.

Anderson JS, Ferguson MA, Lopez-Larson M, Yurgelun-Todd D. 2011. Connectivity gradients between the default mode and attention control networks. Brain Connect 1:147–157.

Andrews-Hanna JR, Reidler JS, Sepulcre J, Poulin R, Buckner RL. 2010. Functional-anatomic fractionation of the brain's default network. Neuron 65:550–562.

Britz J, Landis T, Michel CM. 2009. Right parietal brain activity precedes perceptual alternation of bistable stimuli. Cereb Cortex 19:55–65.

Buckner RL, Andrews-Hanna JR, Schacter DL. 2008. The brain's default network: anatomy, function, and relevance to disease. Ann N Y Acad Sci 1124:1–38.

Chadick JZ, Gazzaley A. 2011. Differential coupling of visual cortex with default or frontal-parietal network based on goals. Nat Neurosci 14:830–832.

Corbetta M, Shulman GL. 2002. Control of goal-directed and stimulus-driven attention in the brain. Nat Rev Neurosci 3:201–215.

Dosenbach NU, Fair DA, Miezin FM, Cohen AL, Wenger KK, Dosenbach RA, Fox MD, et al. 2007. Distinct brain networks for adaptive and stable task control in humans. Proc Natl Acad Sci USA 104:11073–11078.

Fox MD, Snyder AZ, Vincent JL, Corbetta M, Van Essen DC, Raichle ME. 2005. The human brain is intrinsically organized into dynamic, anticorrelated functional networks. Proc Natl Acad Sci U S A 102:9673–9678.

Friston KJ, Buechel C, Fink GR, Morris J, Rolls E, Dolan RJ. 1997. Psychophysiological and modulatory interactions in neuroimaging. Neuroimage 6:218–229.
Friston KJ, Harrison L, Penny W. 2003. Dynamic causal modelling. Neuroimage 19:1273–1302.
Greicius MD, Krasnow B, Reiss AL, Menon V. 2003. Functional connectivity in the resting brain: a network analysis of the default mode hypothesis. Proc Natl Acad Sci U SA 100: 253–258.
Grill-Spector K, Kourtzi Z, Kanwisher N. 2001. The lateral occipital complex and its role in object recognition. Vision Res 41:1409–1422.
Gusnard DA, Raichle ME, Raichle ME. 2001. Searching for a baseline: functional imaging and the resting human brain. Nat Rev Neurosci 2:685–694.
Hirsch J, Egner T, Khalil D, Lai G, Patel A. 2004. Long-range cortical systems and local parietal areas engaged during the multiple percepts of bistable figures suggest a role for "highly influential" neural ensembles in perceptual grouping mechanisms: an fMRI investigation. J Vis 4: Article 245.
Kastner S, Ungerleider LG. 2000. Mechanisms of visual attention in the human cortex. Annu Rev Neurosci 23:315–341.
Kelly AM, Uddin LQ, Biswal BB, Castellanos FX, Milham MP. 2008. Competition between functional brain networks mediates behavioral variability. Neuroimage 39:527–537.
Kleinschmidt A, Büchel C, Zeki S, Frackowiak RS. 1998. Human brain activity during spontaneously reversing perception of ambiguous figures. Proc Biol Sci 265:2427–2433.
Leopold DA, Logothetis NK. 1999. Multistable phenomena: changing views in perception. Trends Cogn Sci 3:254–264.
Malach R, Reppas JB, Benson RR, Kwong KK, Jiang H, Kennedy WA, Ledden PJ, et al. 1995. Object-related activity revealed by functional magnetic resonance imaging in human occipital cortex. Proc Natl Acad Sci U S A 92:8135–8139.
McLaren DG, Ries ML, Xu G, Johnson SC. 2012. A generalized form of context-dependent psychophysiological interactions (gPPI): a comparison to standard approaches. Neuroimage 61:1277–1286.
Meng M, Tong F. 2004. Can attention selectively bias bistable perception? Differences between binocular rivalry and ambiguous figures. J Vis 4:539–551.
O'Reilly JX, Woolrich MW, Behrens TE, Smith SM, Johansen-Berg H. 2012. Tools of the trade: psychophysiological interactions and functional connectivity. Soc Cogn Affect Neurosci 7:604–609.
Penny WD, Stephan KE, Mechelli A, Friston KJ. 2004. Comparing dynamic causal models. Neuroimage 22:1157–1172.
Raichle ME, MacLeod AM, Snyder AZ, Powers WJ, Gusnard DA, Shulman GL. 2001. A default mode of brain function. Proc Natl Acad Sci U S A 98:676–682.
Rees G, Kreiman G, Koch C. 2002. Neural correlates of consciousness in humans. Nat Rev Neurosci 3:261–270.
Schröder H. 1858. Ueber eine optische Inversion bei Betrachtung verkehrter, durch optische Vorrichtung entworfener physischer Bilder. Annalen der Physik und Chemie 181:298–311.
Shmuel A, Yacoub E, Pfeuffer J, Van de Moortele PF, Adriany G, Hu X, Ugurbil K. 2002. Sustained negative BOLD, blood flow and oxygen consumption response and its coupling to the positive response in the human brain. Neuron 36:1195–1210.
Slotnick SD, Yantis S. 2005. Common neural substrates for the control and effects of visual attention and perceptual bistability. Brain Res Cogn Brain Res 24:97–108.
Spreng RN, Stevens WD, Chamberlain JP, Gilmore AW, Schacter DL. 2010. Default network activity, coupled with the frontoparietal control network, supports goal-directed cognition. Neuroimage 53:303–317.
Sterzer P, Kleinschmidt A, Rees G. 2009. The neural bases of multistable perception. Trends Cogn Sci 13:310–318.
Tong F, Nakayama K, Vaughan JT, Kanwisher N. 1998. Binocular rivalry and visual awareness in human extrastriate cortex. Neuron 21:753–759.
Toppino TC, Long GM. 1987. Selective adaptation with reversible figures: don't change that channel. Percept Psychophys 42:37–48.
Uddin LQ, Kelly AM, Biswal BB, Xavier Castellanos F, Milham MP. 2009. Functional connectivity of default mode network components: correlation, anticorrelation, and causality. Hum Brain Mapp 30:625–637.
Wade AR. 2002. The negative BOLD signal unmasked. Neuron 36:993–995.

Address correspondence to:
Joy Hirsch
Department of Psychiatry and NeuroBiology
Brain Function Laboratory
Yale University School of Medicine
300 George St, Suite 902
New Haven, CT 06511

E-mail: joy.hirsch@yale.edu;
joyhirsch@yahoo.com